ELSEVIER

Journal of Molecular Catalysis A: Chemical 96 (1995) 123–143

JOURNAL OF MOLECULAR CATALYSIS A: CHEMICAL

Use of NMR techniques for studying deactivation of zeolites by coking

J.L. Bonardet, M.C. Barrage, J. Fraissard

Laboratoire de Chimie des Surfaces, URA-CNRS 1428, Université P. et M. Curie 4 Place Jussieu, Paris 75252 Cédex 05, France

Received 7 October 1994; accepted 12 October 1994

Abstract

NMR occupies an important place in the study of the deactivation of zeolites by coking. Indeed, association of the resonances of several nuclei has shown that it is possible to investigate: the nature of the carbonaceous deposits; under certain conditions, the coke content; the mode of zeolite deactivation; the exact location of the internal coke and the evolution of its distribution with the coke content, the presence of carbonaceous residues at the crystallite surface; the effect of zeolite structure and the nature of the reactant on coking and regeneration. It also reveals the role of extraframework aluminium species and that of certain lattice Al atoms in the coking process.

Keywords: Coking; Deactivation; NMR spectroscopy; Zeolites

1. Introduction

The deactivation of catalysts, especially zeolites, during cracking, hydrocracking, methanol conversion, etc., is one of the major technological and economic problems of the chemical industry [1]. The interest in these materials lies not only in their high catalytic activity and selectivity but also in the possibility of regenerating them several times so that their 'lifetime' is compatible with the cost of their production. Consequently, it is necessary to understand the manner and the rate of catalyst deactivation as well as the nature of the carbonaceous residues formed, commonly called 'coke'. This generic term covers all sorts of organic materials deposited on a catalyst during a reaction and causing its deactivation. Many studies [2–6] have been performed in order to determine the nature and the composition of the coke (a complex mixture of carbon compounds, polyaromatic or not; we shall speak of coke 'molecules' though well aware that this is generally incorrect), its mode of formation (nature of the precursors), its location (in the zeolite crystallites or at the external surface of the zeolite) and the mode of deactivation of the zeolite (blockage of pores or poisoning of the active sites). The general conclusion is that the formation of carbonaceous deposits and their action upon the zeolites depend on their pore structure, the nature of the reactants involved and the experimental conditions (reaction temperature, reactant pressure, etc). By example the very rapid deactivation of H-mordenite is related to its one-dimensional structure. The presence of a coke molecule in a channel makes all the active sites in the channel inaccessible to the reactants [5,7]. In this case there is pore blockage. As regards HY and H-ZSM-5 zeolites,

SSDI 1381-1169(94)00030-1

although they both have a three-dimensional lattice, the nature and the formation of coke, and the rates of coking and deactivation are very different [6]. One cannot therefore attribute the deactivating effect of coke simply to pore blockage. This effect is more pronounced for HY than for H-ZSM-5 [5]. This can be explained by a heterogeneous distribution of the coke, which attaches itself initially to the strongest acid sites of HY [8] causing their deactivation. In the case of H-ZSM-5, in which all the active sites are equally strong [9], coking is homogeneous and the deactivation is directly related to the coke concentration [6].

The many techniques which have been developed to study coking can be classified as follows:

(i) Chemical: the adsorption of molecules of different sizes gives information about the location of the coke [5]; solvent extraction [10] is used to identify its chemical nature.

(ii) Physical: X-ray diffraction [11] and electron microscopy [12] (coke location); EPR [13] (existence of paramagnetic centres); IR [14] (chemical nature of coke, variation of the concentration of active sites during deactivation): NMR [8,15–18] (nature, location, involvement of the lattice in deactivation, variation of the number of active acid sites, etc.).

Among these techniques, NMR occupies a particularly important place because of the diversity of the nuclei which can be studied (^{13}C, ^{27}Al, ^{29}Si, ^{1}H and ^{129}Xe) and the development of high resolution solid NMR. For this reason, in this article we shall make a special effort to demonstrate its advantages and the contribution of each of the nuclei listed above to the understanding of the phenomenon of coking.

2. Study of zeolite coking by ^{13}C–MAS–NMR

The first nucleus used to characterise the nature of the carbonaceous residues formed in zeolites was of course ^{13}C. The development of sophisticated techniques such as magic angle spinning (MAS) and crossed polarisation (CP) as well as the use of strong magnetic fields amply compensates for the low natural abundance (1%) and the low detection sensitivity ($10^{-2}/^{1}H$) of this nucleus. Moreover, the observed chemical shifts are large (0–300 ppm), which makes it easy to distinguish the different types of coke formed (paraffinic, olefinic, aromatic, polyaromatic). It must be noted however that the use of crossed polarisation makes quantitative analysis more difficult. Most of the ^{13}C NMR studies on coking concern Y and ZSM-5 zeolites, since these are catalysts greatly used in the chemical industry, the first for the cracking of heavy oils obtained by fractional distillation of crude oils, the second particularly for the transformation of methanol into gasoline. Because they are easy to use, large-pore acid zeolites may be preferred to concentrated sulphuric acid or anhydrous hydrofluoric acid as catalysts in the production of high-octane gasoline by alkylation of isobutane with light olefins. However, their selectivity decreases rapidly, doubtless due to poisoning of the strongest acid sites by carbonaceous deposits [25].

Derouane et al. [17] were the pioneers of this type of study, since as of 1982 they used this technique to identify carbonaceous deposits formed in situ on zeolites during methanol conversion (in the presence of H-ZSM-5 and H-mordenite) and that of ethylene (on H-ZSM-5). The nature of these residues depends both on the type of zeolite and on the reactant. Thus, the conversion of methanol on H-ZSM-5 leads to a wide distribution of aliphatic compounds ($10 < \delta < 40$ ppm) and to some aromatic compounds ($125 < \delta < 145$ ppm) (benzene, toluene and xylene) and to straight-chain and branched olefins (δ about 150 ppm) (Fig. 1-a). The isoparaffins are more abundant than straight-chain paraffins, in agreement with classical data on the conversion of methanol on H-ZSM-5 [19]. On H mordenite it leads to a distribution more limited in aliphatics $13 < \delta < 25$ ppm) (no isoparaffins) but broader in aromatics (130–170 ppm), (Fig. 1-b) including polyaromatics. The absence of aliphatics with 5 carbon atoms and isoparaffins is a result of the large pore size, which facilitates the conversion of C4 and

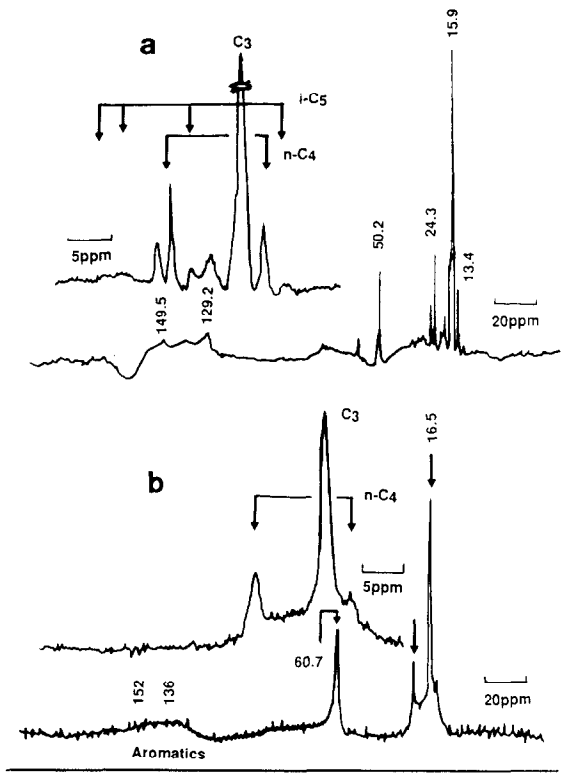

Fig. 1. CP/MAS–13-C NMR spectra of the carbonaceous deposits from the catalysed methanol conversion to hydrocarbons by: (a) zeolite H-ZSM-5; (b) zeolite H-Mordenite. (adapted from [17]).

C6 olefins to aromatics [21] and also the formation of polyaromatics, as has been shown by Walsh and Rollmann [20].

To prove the dependence between the reactant, the operating conditions and coke formation, Derouane et al. [22] studied the conversion of ethylene under various experimental conditions. On dehydrated H-ZSM-5 zeolite, ethylene reacts rapidly at ambient temperature to give a straight-chain polymer (Fig. 2-a). The adsorption of water followed by treatment at 573 K leads to high molecular weight polymer cracking products (Fig. 2-b).

These first results obtained by ^{13}C CP/MAS NMR make it possible therefore to show how the nature of the carbonaceous deposits depends on the zeolite structure, the type of reactant involved and the operating conditions, but they do not distinguish between coke inside the crystallites and that deposited on the external surface. Moreover, the in situ study does not allow a distinction between the reaction products and the carbonaceous deposits.

On the other hand, Lange et al. [23] several years later, made it possible to perform in situ experiments without confusing the reaction products and the coke deposits. They studied by IR and ^{13}C NMR spectroscopy the steps in the formation of coke during the conversion of ethylene on H-mordenite zeolites as a function of the temperature. The ^{13}C MAS NMR results show that there are two types of coke: low-temperature coke formed after adsorption at 298 K, then heating to $T \leq 500$ K, and high-temperature coke ($T > 500$ K) (Fig. 3). At 298 K, after ethylene adsorption straight-chain ($\delta = 13$, 25, 30–33 ppm) and branched ($\delta = 40$ ppm) paraffinic oligomers are formed: the active terminal groups are of the alkoxide type ($\delta \leq 50$ ppm), while Derouane et al. [22] did not observe a peak at 50 ppm in the

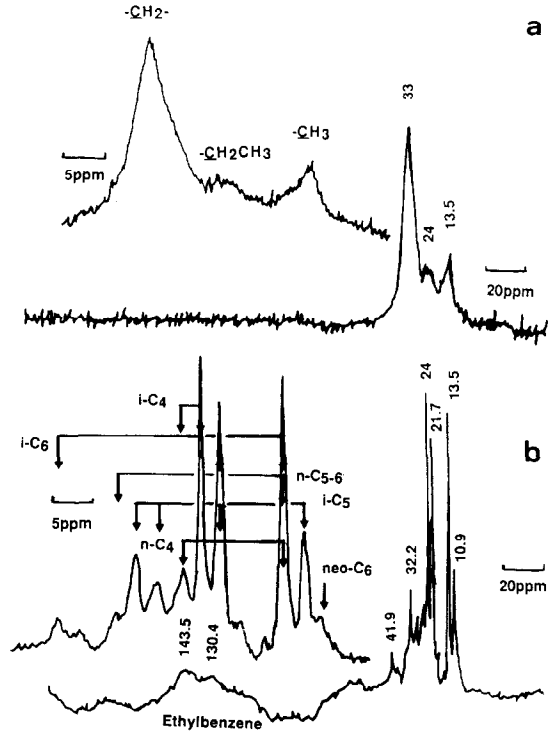

Fig. 2. CP/MAS–13-C NMR spectra of: (a) H-ZSM-5 following ethylene adsorption and oligomerisation at 295 K, (b) the carbonaceous deposits from the cracking in the presence of steam (573 K) of an ethylene oligomer ($n = 5$–6) (adapted from [22]).

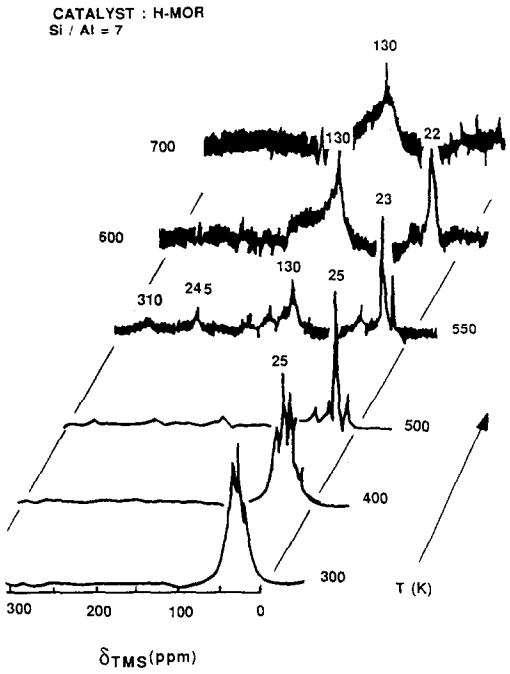

Fig. 3. 13-C–MAS–NMR spectra of carbonaceous deposits formed by reaction of ethene over H-Mordenite (from [23]).

oligomerisation of ethylene at ambient temperature on H-ZSM-5 zeolite. When the previous sample is heated to 500 K the carbonaceous deposits isomerise and crack to give smaller paraffinic molecules ($\delta = 9$, 20–24 ppm). During the transition of low-temperature coke to high-temperature coke (at about 500 K) the reaction intermediates are then alkyl ($\delta = 310$ ppm), allyl ($\delta = 130$ to 150 ppm) and protonated aromatic ($\delta = 130$–150 ppm) carbocations. At and above 550 K the coke consists of alkylbenzene and small polynuclear aromatics ($\delta = 185$ and 130 ppm). These authors also showed that the formation of low-temperature coke ($T < 500$ K) during the conversion of ethylene on H-mordenite is not affected by a change in the aluminium content, contrary to high-temperature coke ($T > 500$ K). In this latter case, C1 to C4 alkanes are formed only on dealuminated zeolites.

White et al. [24] also showed that high-temperature cracking reactions can be studied in situ. After adsorption of propene-1-^{13}C or propene-2-^{13}C at ambient temperature on HY zeolite very branched oligomers are formed. The mechanism proposed involves an alkoxide intermediate, indicated by the peak at 87 ppm after adsorption of propene-2-^{13}C (Fig. 4-a). The sealed samples are then heated. These oligomers begin to crack at 503 K. The ^{13}C MAS NMR signals correspond to very mobile low molecular weight alkanes (propane and branched C4 to C6 alkanes) (Fig. 4-b). Moreover, by combining MAS and cross polarization they demonstrated the formation of aromatic coke when propene oligomers are cracked at temperature above 500 K (Fig. 4-c). Since these experiments are carried out in a closed system the authors conclude that coking supplies the hydrogen atoms necessary to form acyclic alkanes during the cracking of the oligomers.

In situ studies performed under certain conditions make it possible therefore avoid the confu-

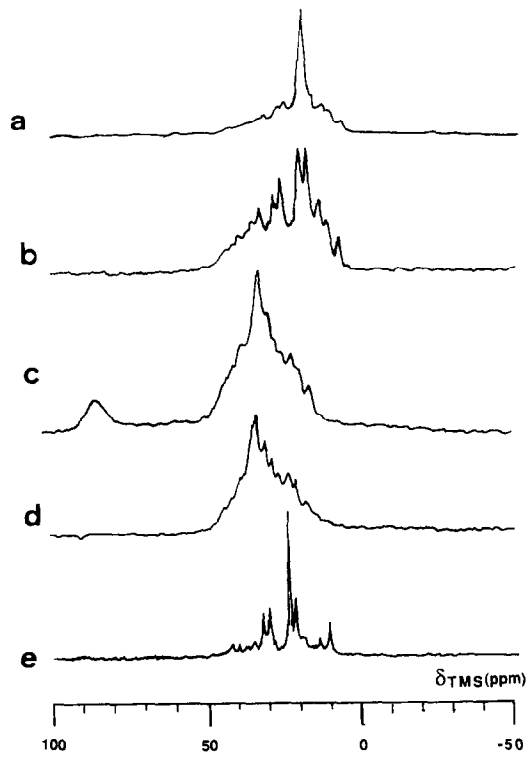

Fig. 4. 13-C–MAS–NMR spectra of oligomers formed from labelled propene on zeolite HY: (a) CP spectrum of the oligomers of 1-^{13}C at 298 K prior to heating. (b) Bloch decay spectrum of the sample in a. (c) CP spectrum of the oligomers of 2-^{13}C at 298 K prior to heating. (d) Bloch decay spectrum of the sample in a. (e) Bloch decay spectrum of the sample in c and d at 298 K after 3 h at 503 K (from [24]).

sion between the reaction products and the carbonaceous deposits: they provide a certain number of new elements towards the understanding of the coking phenomenon, such as the detection of reaction intermediates depending on the temperature.

Industry often uses NaY zeolites partially exchanged with rare earths, since these exchanged zeolites are more stable at high temperature. For this reason, various authors have examined the formation of coke on such zeolites. Weitkamp and Maixner [26] established that the nature of the coke deposited on a LaNaY zeolite from the alkylation of isobutane with 1-butene depends on the reaction temperature. At 353 K, a typical temperature for alkylation, the carbonaceous deposits are solely paraffins. When the temperature increases they change and one finds more and more olefins and aromatics (Fig. 5).

For Maixner et al. [18] the chemical nature of the carbonaceous deposits in a LaNaY zeolite depends on the conditions of their formation, the most important parameters being the reaction temperature and the nature of the reactant. They studied the conversion of three types of reactants: an aromatic, toluene; an alkene, 1-hexene; an alkane, 2,2,4-trimethylpentane, at various reaction temperatures. Whatever the temperature, the amount of coke in the conversion of 1-hexene is always high; at low temperature (373 K) the carbon residues are isoparaffins ($\delta = 16$, 25 and 31 ppm), while at higher temperature they are olefins and alkylaromatics ($\delta \approx 110$–150 ppm) (Fig. 6-a). On the other hand, toluene is relatively unreactive: at 373 K it is not converted; its conversion is constant (7%) at 632 K. The carbon deposits then formed are essentially polyaromatic compounds ($\delta = 110$–150 ppm) (Fig. 6-b). At 373 K the carbon compounds obtained from the alkane are essentially paraffins ($\delta = 13$–30 ppm), with little in the way of olefins or aromatics ($\delta = 110$–150 ppm). When the temperature increases the amount of aromatic coke increases (Fig. 6-c).

This work claims that the nature of the coke deposited on Y zeolites depends on the reactant used and on the reaction temperature but, regardless of the reactant, a high temperature favours the formation of aromatic coke.

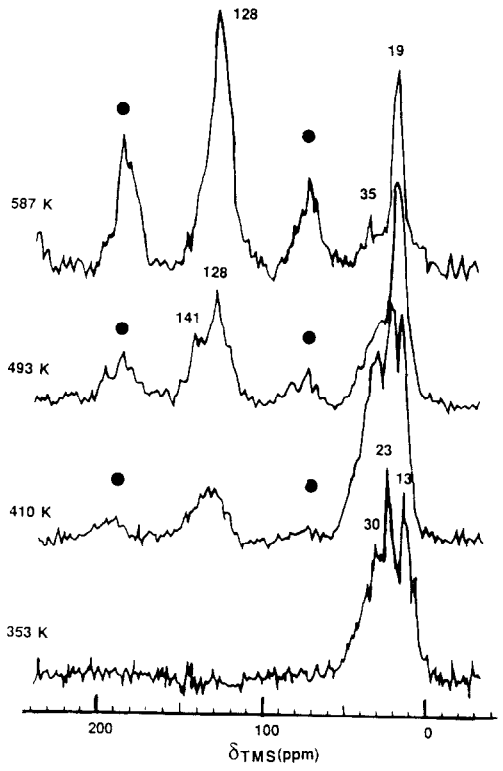

Fig. 5. CP/MAS–13-C NMR spectra of the carbonaceous deposits from the conversion of isobutane and 1-butene on LaNaY zeolite at different temperatures. (●) Spinning sidebands (from [26]).

This result was confirmed by Richardson and Haw [27] who demonstrated that the aromaticity of the coke deposited on HY zeolites during butadiene conversion depends also on the reaction temperature: the carbonaceous deposits for samples coked at a temperature equal to or greater than 773 K are totally aromatic or graphitic. Moreover, they used the spin counting technique to evaluate the reaction temperature up to which the ^{13}C/CP/MAS NMR spectra can be analysed quantitatively. These experiments were performed by the method described by Hagaman et al. [28], which consists in recording the spectra of a measured quantity of a sample mixed with a known amount of glycine. From the percentage by weight of carbon contained in the zeolite (obtained by elemental analysis) and integration of the intensities of the glycine and the coke it is

possible to calculate the fraction of carbon which can be detected by NMR (a correction factor is used for the integrated intensities of glycine and coke, since the inequality: $t_{CH} \ll$ contact time $\ll t_{1\rho}(H)$ is not satisfied. t_{CH} is the time constant for the transfer of the magnetisation of the protons to ^{13}C and $t_{1\rho}(H)$ is the longitudinal relaxation time of ^{1}H in the rotating frame). These experiments reveal that at very low reaction temperature the ^{13}C/CP/MAS NMR spectra can be analysed quantitatively. However, as the temperature increases the fraction of aromatic carbon atoms is underestimated; already at 423 K only 78% of the C is detected by NMR. This is due to the presence of organic free radicals (which cause considerable broadening of the signals) and of proton-deficient regions (CP is inefficient in the graphitic region). The authors conclude that ^{13}C/CP/MAS NMR cannot be used to determine the coke level in HY zeolites when the reaction temperature is above 423 K.

Munson and Haw [29] also tested the effect of rare earth cations on the efficiency of this technique for the quantitative characterisation of the coke contained in rare earth HY zeolites. The carbonaceous deposits on these samples are obtained by the conversion of propene at 473 K. The lanthanides are in general paramagnetic; they can cause a considerable decrease in the transversal relaxation time of ^{13}C, i.e. a broadening of the ^{13}C resonances and also markedly decrease $t_{1\rho}$ reducing the efficiency of cross.polarization.

Measurements of relaxation time and spin counting indicate that the coke deposits on industrial lanthanide-HY (La or Nd) samples can be characterised by this technique, whereas small amounts of Gd^{3+} and Dy^{3+} cations, which have long spin-lattice relaxation times, have a harmful effect on the determination of the percentage of carbon atoms from ^{13}C/CP/MAS NMR spectra.

This work therefore indicates the limits of the quantitative determination of the percentage of coke deposited in Y zeolites from ^{13}C/CP/MAS NMR spectra.

Other authors have shown these limits for ZSM-5 zeolites. Thus Meinhold and Bibby [30] studied

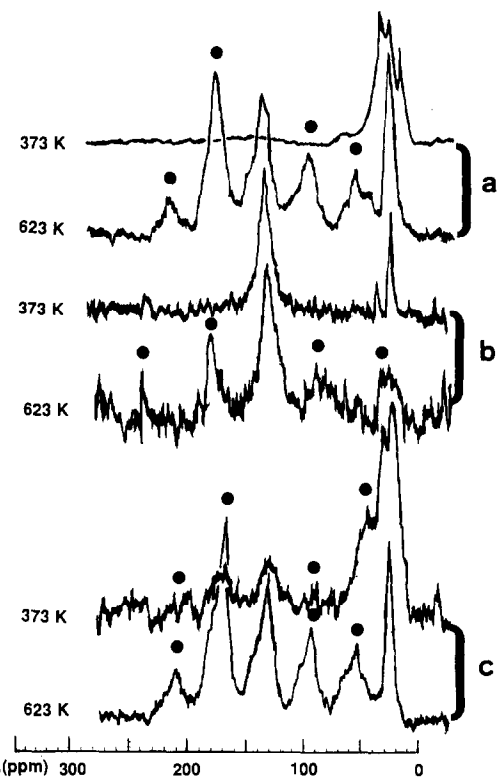

Fig. 6. CP/MAS–13-C NMR spectra of the carbonaceous deposits from the conversion of 1-hexene (a), toluene (b) and 2,2,4-trimethylpentane (c) on LaY zeolite. (●) Spinning sidebands. (adapted from [18]).

samples of H-ZSM-5 zeolites more or less coked during the conversion of methanol to petrol. They compared them with samples where the coke deposited on the external surface of the crystallites had been selectively removed by treatment in a low pressure oxygen plasma. Their results show that only part of the carbon atoms is detected by NMR and that the percentage of carbon atoms 'visible' decreases when the amount of coke increases. All the coke is detected below a coke content of 0.85% (in what follows, this is expressed in weight with respect to the initial sample). For the highest coke content (23.6%) only 29% of the coke atoms are visible by NMR (Fig. 7). The loss of part of the carbon signal can be due to the low values of the transversal relaxation time of the proton and/or to the formation of conducting graphitic structures at the external surface of the zeolite crystallites, which detunes the probe.

These structures contain electrons delocalised on aromatic rings and paramagnetic centres characteristic of defects in the structure of the highly condensed coke [31]; being proton deficient, they cannot be detected by cross polarization. The coke which can be detected by NMR is essentially inside the zeolite channels. At low coke content they are aromatic species, such as benzene and methyl-substituted naphthalene. When the coke content increases these species condense to form polycyclic aromatic compounds and the extent of methyl substitution decreases. Some polyaromatic species could be present in small amounts at the surface, but at high coke content the surface species appear to be mainly graphitic and therefore invisible to NMR. They block the openings of the pores on the surface and hinder the diffusion of the methanol in the channels and that of the products out of the channels.

Comparing the results of Derouane et al. [17] with those of Meinhold and Bibby [30] we observe that studying the same reaction by the same technique leads to different results (wide distribution of aliphatic compounds and a few aromatic compounds for the former and essentially aromatic species for the latter). However, Derouane et al. did not eliminate the reaction products before spectral analysis nor were the experimental conditions identical, which confirms that the nature of the carbonaceous deposits depends to a large extent on the reaction conditions [3].

Moreover, the above study proves that beyond 1% w/w of coke ^{13}C/CP/MAS NMR can no longer be used to determine quantitatively the amount of coke deposited on a ZSM-5 zeolite.

Others such as Ernst et al. [16,32] have considered the effects of dealumination on the ^{13}C/CP/MAS NMR spectra of H-ZSM-5 zeolites coked during n-hexane cracking. These samples were dealuminated by steaming. The spectrum of the non-dealuminated sample contains two fairly broad peaks, one in the region of aliphatic species ($\delta = 20$ ppm) and the other, larger one, in the range of aromatic species ($\delta = 130$ ppm) (Fig. 8) while the spectrum of the dealuminated samples contains only one signal, attributed to aromatic

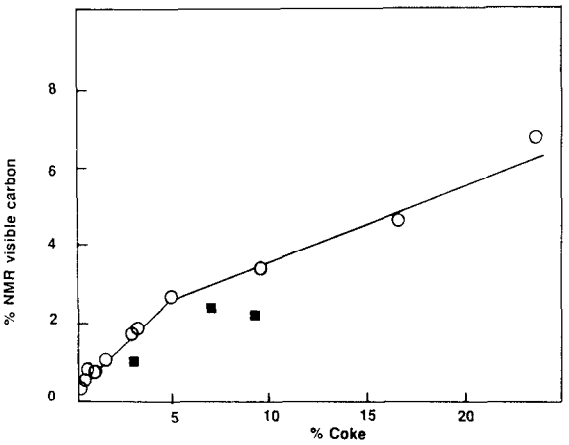

Fig. 7. Percentage of carbon in H-ZSM-5 catalyst detected by NMR versus coke content. (■) RF oxygen plasma-treated samples (from [30]).

compounds. These authors also estimated the coke content of various slightly coked samples and showed further [33] that the catalytic activity of the dealuminated samples is greater than that of the initial samples. The ^{13}C NMR results indicate that the increased catalytic activity of the dealuminated samples does not increase the coke content and that these deposits are essentially aromatic.

These conclusions regarding the chemical nature of the carbonaceous deposits are consistent with those of Meinhold and Bibby [30] who showed that beyond a certain coke content the carbon compounds were polyaromatics and that the degree of methyl substitution decreased.

The above authors were not concerned with reaction intermediates formed briefly during coking. On the other hand, Bosacek et al. [34] suggest that phenoxy groups are formed at the surface of H-ZSM-5 zeolite coked during the conversion of acetone (various reaction products). The signal at 154 ppm in the ^{13}C NMR spectrum (Fig. 9) was considered to be characteristic of these phenoxy groups. Indeed, bromine vapour at 298 and 373 K does not modify the spectra of these coked samples: there are therefore no olefinic carbons; moreover, partial oxidation of the coke at temperatures above 773 K leads to no significant change in the spectrum: the creation of carbocations as transitory species therefore appears unlikely. Upon

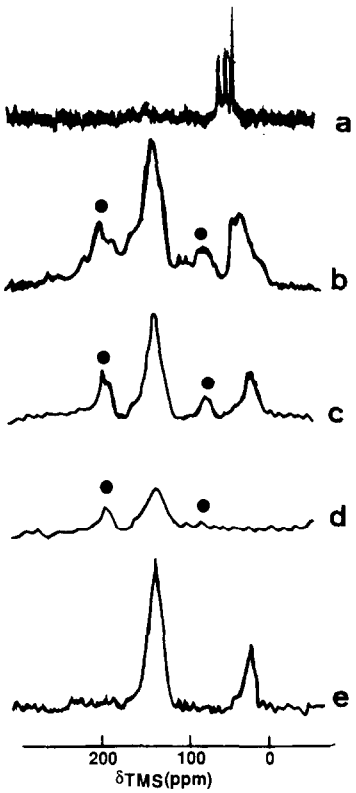

Fig. 8. 13-C–MAS–NMR spectra of the samples coked by n-hexane cracking: (a) H-ZSM-5/0 before heating at 673 K; (b, c, d) H-ZSM-5/0, 10, 40 after heating the samples up to 673 K; (e) the same as b but after suppression of the spinning sidebands (TOSS method). 0, 10, 40 denote the water pressure in kPa during hydrothermal treatment. (●) Spinning sidebands (from [32]).

pyrolysis under vacuum at 873 K the peak at 19.8 ppm disappears, indicating that there is dealkylation, but the signal at 154 ppm is unaffected (Fig. 9-c).

In the case of acetone conversion on a large-pore zeolite (HY), however, condensation to polyaromatics occurs (large shoulder at 140 ppm), the signal at 154 ppm being absent.

By using both chemical treatment and ^{13}C NMR, Carlton et al. [35] showed that aromatic coke is the only type directly involved in the deactivation of ZSM-5 zeolite. Catalyst regeneration by oxygen leads to the progressive elimination of the aliphatics and the aromatics; with an ozone/oxygen mixture only the aromatics are eliminated. This is probably due to attack on the unsaturated centres of the coke, leading to oxygen-containing fragments. This result is confirmed by the broadening of the resonance signal corresponding to ethers (60–125 ppm). Catalyst deactivation is caused by the aromatic coke, since the aliphatics, the ethers and the ketones in the zeolite can be tolerated without significant deactivation.

2.1. Conclusion.

The data provided by ^{13}C NMR concern primarily the chemical nature of the coke. This depends on the porous structure of the zeolites, on the nature of the reactant and on the reaction temperature. The results analysed above indicate that beyond a certain percentage of coke or beyond a certain reaction temperature the carbonaceous deposits are essentially polyaromatic (and that their concentration increases with the coke content on the temperature) both on Y and ZSM-5 zeolites or mordenite, this being the case regardless of the reactant.

Other information can be provided by ^{13}C NMR, such as the demonstration of the existence of reaction intermediates responsible for the formation of coke.

However, there are certain disadvantages to this technique: (i) the coke content of the samples can be estimated only for lightly coked zeolites (or zeolites coked at low temperature): chemical analysis has to be used to determine the percentage of coke deposited: (ii) the nature of the coke can be determined but this method does not distinguish between coke located in the cages or channels and that on the external surface of the zeolite crystallites.

3. Study of zeolite coking by ^{29}Si and ^{27}Al NMR

^{29}Si CP/MAS and ^{27}Al MAS NMR are less used than 13-CP/MAS NMR to study coking. Nevertheless, they have a certain interest since they can be used to determine the effect of coking on the zeolite lattice.

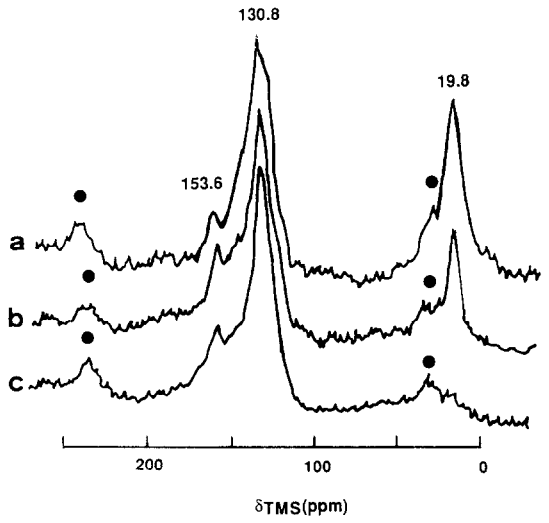

Fig. 9. ^{13}C/CP/MAS NMR spectra of the carbonaceous deposits after acetone reaction on H-ZSM-5 zeolite: (a) 10% of coke; (b) sample a after partial oxidation at 473 K; (c) sample b after pyrolysis at 873 K for 2 h. (●) Spinning sidebands (from [34]).

Most authors have associated these two techniques, since they are complementary. Filling the channels with carbonaceous deposits modifies both the ^{27}Al and ^{29}Si NMR spectra. Thus, Meinhold and Bibby demonstrated [36] that they can be used to estimate the volume occupied by the coke in H-ZSM-5 zeolites coked in the conversion of methanol at 643 K, as well as the proton content of the coke and, consequently, the size of the coke 'molecules'. ^{29}Si/CP/MAS NMR allows the measurement of the proton content of coke and therefore of the C/H ratio. For this purpose the intensities of the ^{29}Si signal are compared with the results obtained by the authors for the adsorption of benzene on H-ZSM-5 [37]; an empirical linear relationship between the intensity of the ^{29}Si signal and the hydrogen concentration of the adsorbed benzene was set up. This relationship is valid for coke contents between 0.85 and 9.6%, the number of protons per u.c. given by the coke content being then equivalent to the number of ^{29}Si obtained by CP NMR (Fig. 10).

As for ^{27}Al NMR the increase in the shift and the width of the Al signal, as well as the decrease in its intensity when the amount of coke increases, are very similar to the modification produced by the dehydration of H-ZSM-5 or by the adsorption of alkanes. These modifications are probably due to the effect of an increase in the electric field gradient, which induces quadrupolar shifts and an increase in the transversal relaxation time. The same authors [37] have shown that there is a linear relationship between the position and the width of the Al signal (Fig. 11). By comparing the position, the width and the intensity of the peak for coked samples with those of the initial H-ZSM-5 sample containing various amounts of water, they estimated the amount of water remaining in the channels after coking, in order to determine the average size of the coke molecules. In the same way, the decrease in the longitudinal relaxation rates for ^{29}Si and ^{1}H is due to the replacement of oxygen by coke in the channels. Thus, from the relaxation rate of ^{29}Si (proportional to the amount of oxygen in the channels) these authors were able to measure the volume percentage of oxygen remaining. Their results are in agreement with those obtained by ^{13}C-NMR [30] the carbon compounds in the channels are methyl-substituted polyaromatics. When the coke content is higher than 16% the broadening and the chemical shift observed in the ^{29}Si spectra are interpreted by the authors as being due to a slight

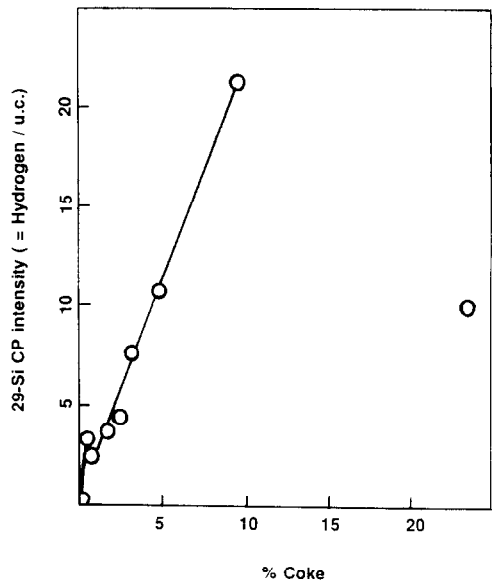

Fig. 10. Effect of coking on the ^{29}Si/CP/MAS NMR intensity as the number of CP–NMR visible silicons/u.c. This has been shown to be equivalent to the hydrogens/u.c. (from [37]).

distortion of the zeolite channels as a result of the formation of more rigid coke molecules, confirming the XPS results of Seyton et al. [38]. In this case ^{29}Si/CP/MAS NMR provides as much information as ^{27}Al–MAS–NMR.

On the other hand Ernst et al. [16] have shown that for slightly dealuminated H-ZSM-5 zeolites, n-hexane cracking does not modify the ^{29}Si/CP/MAS NMR spectra, whereas the intensity of the ^{27}Al signal of the lattice Al atoms decreases. The carbonaceous deposits therefore make it impossible to detect some of the lattice Al atoms. Freude et al. [39] interpret these results in terms of the covering of the Brønsted acid sites by the carbonaceous residues which perturb the tetrahedral symmetry of the Al atoms. They deduce from this that the catalytic deactivation is caused mainly by poisoning of the Brønsted acid sites.

Echevskü et al. [40] considered only ^{27}Al–MAS NMR to determine the role of extraframework Al species (Al_{NF}) in the formation of coke on dealuminated pentasil zeolites in the conversion of methanol to hydrocarbons. To do this, they compared the concentration of Al_{NF} atoms with the deactivation rate of these zeolites after methanol conversion. They demonstrated that there is no direct relationship between the Al_{NF}/Al_F ratio and the deactivation rate. Their results indicate that most of the Al_{NF} species in an octahedral environment are not involved in the formation of carbonaceous deposits and have no effect on the deactivation rate, in contradiction with what was established by Ione et al. [41] for 'large pore' zeolites (Y, mordenite). They deduce from these results that the Al_{NF} species do not favour the formation of coke except in the absence of considerable steric hindrance.

These results appear to contradict those of Bonardet et al. [42] for a dealuminated H-ZSM-5 zeolite coked during acetone conversion, then regenerated by oxidation. The spectrum of the initial sample shows two signals, at 60 ppm (Al_F) and at 0 ppm (Al_{NF}) (Fig. 12). That of the sampled coked to 10.7% w/w shows only a much broadened signal at 60 ppm; the signal at 0 ppm appears only as a shoulder. The spectrum of the

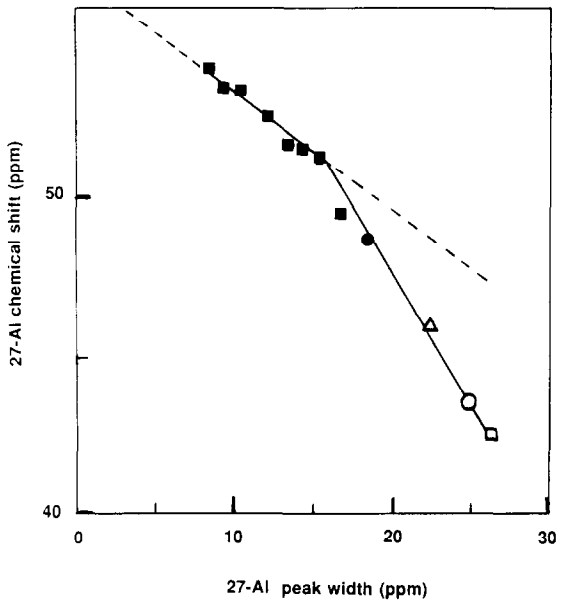

Fig. 11. Relationship between 27-Al chemical shift and 27-Al peak width in coked H-ZSM-5: (■) 0–10% coke; (●) 16.5% coke; (■) 23.6% coke; (○) dehydrated H-ZSM-5 ($1H_2O$/u.c.); (□) fully dehydrated H-ZSM-5. (from [38]).

partially reoxidised sample containing 5.5% of residual coke presents again 2 signals, but the relative intensity of the signal at 0 ppm is weaker than that of the non-coked sample. The disappearance and the reappearance of the 0 ppm signal, attributed to Al_{NF} species in an octahedral environment, led the authors to conclude that these extraframework species are partly involved in the formation of the coke in H-ZSM-5. These results were confirmed by the ^{129}Xe NMR of adsorbed xenon [68].

These authors also studied dealuminated HY samples coked by n-hexane cracking. The spectra of the samples coked from the washed and steamed sample presents three peaks, at 60 (A), 0 (B) and 30 ppm (C); and the relative intensity of C increases with the coke content. The spectrum of the steamed and washed samples shows only two signals, A and B (Fig. 12). The 30 ppm signal has been attributed to Al species of the very deformed and fragile lattice [43,44]. Thus the appearance of signal C after coking and the increase in its relative intensity when the coke content increases proves that coke formation

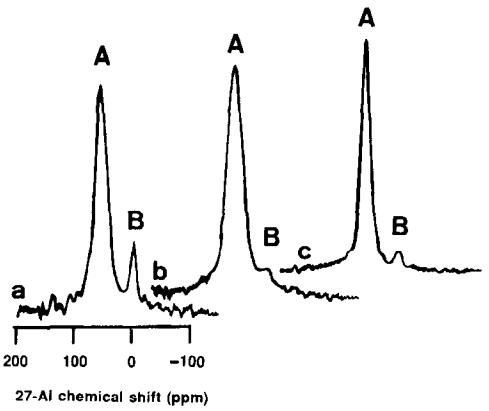

Fig. 12. 27-Al–MAS NMR spectra of H-ZSM-5 zeolites coked during acetone conversion: (a) 0% coked; (b) 10.7% coked; (c) partially oxidized, 5.5% coked (from [42]).

causes fragility of some of the Al_F. This result explains the additional dealumination of the lattice after total regeneration of coked HY zeolites by oxidation [45]. They therefore conclude that for a fairly high coke content certain Al atoms of the lattice are involved in the formation of carbonaceous deposits.

3.1. Conclusion.

First of all, ^{27}Al NMR makes it possible to determine the number of extraframework Al and thus to compare the behaviour of more or less dealuminated zeolites with respect to coking. It is then possible to assess the role of these species in the phenomenon of coking. It can also be used to study the role of lattice Al atoms.

Used in conjunction with ^{29}Si/CP/MAS NMR, it can be used to estimate the volume occupied by the coke in the crystallites and, consequently, the size of the coke molecules, which is correlated with the proportion of methyl-aromatics.

Used in conjunction also with catalytic activity measurements it can indicate the mode of catalyst deactivation (acid site poisoning or pore blockage).

4. Study of coking by ^1H MAS NMR

^1H-MAS NMR can also provide interesting information, notably about the number of Brønsted acid sites still active after coking. In the same way, measurements of self-diffusion by pulsed field gradient give us information about the location of the coke and the resulting variations in the intra and extra-crystallite diffusion.

^1H above all makes it possible to obtain the H/C ratio when the coke content is known and therefore to define the nature of the carbonaceous compounds deposited in or at the surface of the zeolite crystallites.

Lechert et al. [46] studied HY zeolites dealuminated to different extents and coked by butadiene conversion at 530 K. They compared the adsorption capacities and the proton relaxation time of n-butane and benzene in the non-coked and coked samples. Dealumination has practically no effect on the capacity for adsorption of these two molecules. On the other hand, the decrease in the relaxation times, T_1 and T_2, for the coked samples shows that the reorientation of adsorbed n-butane molecules is severely restrained even though the capacity for adsorption of these molecules is little reduced compared to the initial samples, which suggests that there is a change in the stacking of the molecules in the vicinity of the carbonaceous residues. Conversely, these same relaxation measurements prove that the effect of coking on the mobility of benzene is small, whereas the adsorption capacity decreases markedly. Now, benzene molecules are mainly located at the windows between the cavities and move by rotation about their two-fold axes, accompanied by jumps between neighbouring sites [47]. These results can be understood if more than half the cavities are accessible to the benzene molecules, therefore free. Moreover, the coke content corresponding to a mean value of 10C/cavity and the low H/C ratio (about 0.5) suggest that the carbonaceous compounds are molecules with about 20 carbon atoms, such as coronene. These results are in agreement with the previous conclusion. ^1H relaxation time measurements on the adsorbed molecules therefore allow us to find out the distribution of the coke molecules in the zeolite cavities.

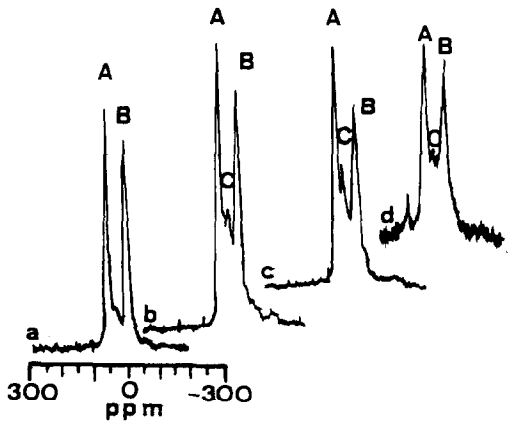

Fig. 13. 27-Al–MAS NMR spectra of Y zeolites after steaming, acid washing and coking by ortho-xylene cracking. (a) Fresh sample; (b) 4.7% coke; (c) 8.7%coke; (d) sample c totally reoxidised (from [45]).

Ernst et al. [32] have used ^{1}H–MAS NMR to estimate the number of Brønsted acid sites still active in slightly dealuminated H-ZSM-5 zeolites coked by n-hexane cracking. The spectra of the non-coked and coked samples are very different (Fig. 14). Peak (a) at 2 ppm corresponds to protons of non-acidic hydroxyl groups (silanols) located at the crystallite surface, at structure defects and in the amorphous parts of the zeolite. The intensity of peak (b) at 4.2 ppm corresponding to the protons of Brønsted acid hydroxyl groups (bridging OH groups) decreases after coking. Moreover, the broad signal (represented by a dotted line for the coked sample) must be caused by the protons of the coke or by the protons of acidic hydroxyl groups which have a strong dipolar interaction with the coke protons. The fall in the intensity of peak (b) allows the calculation of the number of sites still active after coking. This result can be associated with the decrease in the intensity of the ^{27}Al–MAS NMR peak, corresponding to lattice Al atoms, after coking. The authors deduced from these results that the carbonaceous deposits poison the Brønsted acid sites in the zeolite crystallites.

Karger et al. [48] and Volter et al. [49] have used the pulsed field gradient ^{1}H NMR technique to study H-ZSM-5 zeolites coked by n-hexane cracking. These samples are in the form of polycrystalline aggregates or monocrystals. The probe molecule is methane or propane. This technique is used to determine the intracrystalline self-diffusion coefficient of the probe molecules. By measuring the effect of the coke deposit on molecular self-diffusion it is possible to distinguish internal from external coke.

In this technique, introduced by Karger for solids [50], an additional inhomogeneous field, the pulsed field gradient (Fig. 15-b) is superimposed for a short time interval δ on the constant magnetic field B. The first gradient pulse dephases the transversal magnetisation vectors ($M_{\perp}(z)$) in different regions of the sample (Fig. 15-c) and decreases the total transversal magnetisation ($M_{\perp}$) (Fig. 15-d). After a second gradient pulse in the opposite direction, if the molecules diffuse, the total transversal magnetisation decreases. From this decreases it is possible to calculate the intramolecular self-diffusion coefficient $D_i = \langle r^2(\Delta)\rangle/6\Delta$), where Δ is the time between the two gradient pulses and $\langle r^2(\Delta)\rangle$ or r(Δ) rep-

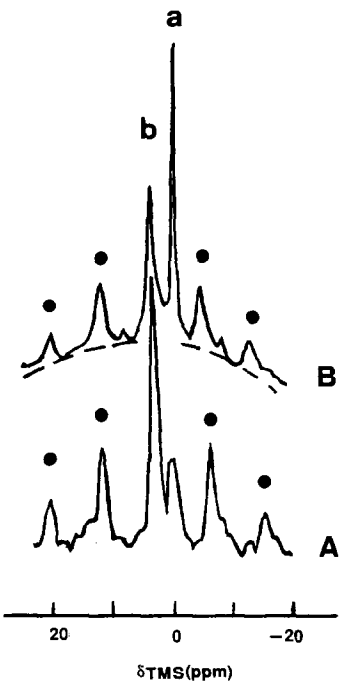

Fig. 14. 1-H–MAS NMR spectra of a non steamed H-ZSM-5 zeolite: (a) before coking; (b) after coking. (●) Spinning sidebands (from [32]).

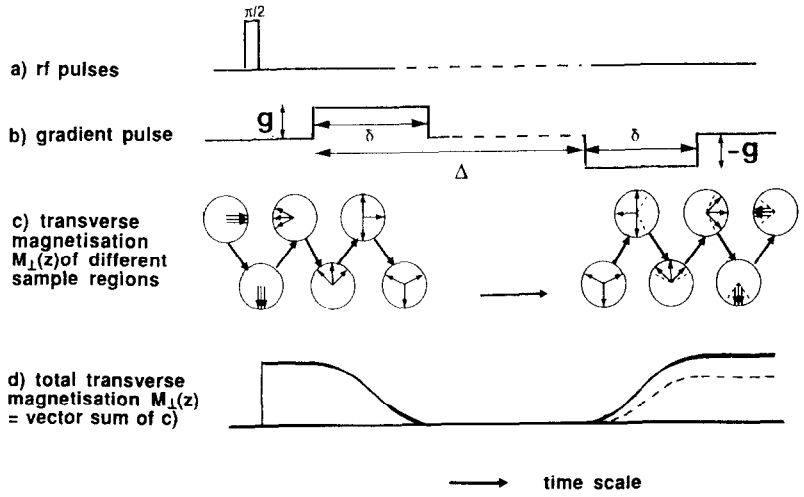

Fig. 15. Schematic representation of a pulse field gradient 1-H NMR experiment. (from [50]).

resents the displacement of a spin during the time Δ. Thus they have proved that the molecular mobility in polycrystalline aggregates is greater than in the initial zeolite monocrystals. After coking, the intracrystalline diffusion of the probe molecule is reduced in all the coked samples; the carbonaceous deposits are therefore inside the crystallites. Moreover, the inhibition of the mobility of methane in the coked polycrystalline aggregates is more pronounced than in the coked monocrystals. The authors deduce from this that the free space between the microcrystals of the aggregates (called the secondary pore lattice, the zeolite channels representing the first-order pores) is preferentially filled by the coke. This technique makes it possible therefore to demonstrate the effect of second-order pores in polycrystalline adsorbants. At high coke content, there is a surface diffusion barrier characteristic of an external coke deposit. They have also shown that the polycrystalline samples are deactivated more slowly than the monocrystals, because of the presence of the secondary pore system in which the coke is deposited without affecting the catalytic activity; the catalyst lifetime is therefore enhanced.

4.1. Conclusion

The H/C ratio can be measured by ^{1}H MAS–NMR when the coke content is known, but this ratio includes all the carbonaceous deposits and is therefore imprecise, since the internal coke is generally very different from the external coke. Under certain conditions it is possible to estimate the number of Brønsted acid sites still active after coking, but it is necessary also to use other resonances (^{27}Al–MAS, for example) in order to reach any conclusion concerning the mode of deactivation. Finally, measurement of the proton relaxation times for probe molecules and pulsed field gradient ^{1}H NMR gives information about the distribution of the carbonaceous deposits in the zeolite crystallites.

5. Study of coking by ^{129}Xe NMR of adsorbed xenon.

^{129}Xe NMR of xenon adsorbed in crystallised microporous solids, developed by Fraissard and Ito at the beginning of the 1980s [52] has proved to be particularly fruitful for the study of certain zeolite properties difficult to handle by classical physicochemical methods; for example, short-range crystallinity and structure defects.

The information provided by the xenon probe is obtained generally by inspection of the $\delta = f(n)$ curve, where n is the number of xenon atoms adsorbed per gram of anhydrous solid. Fraissard et al. [52,53] established that, as for the gas phase,

the chemical shift of adsorbed xenon is the sum of several terms corresponding to the various perturbations to which it is subjected:

$$\delta = \delta_0 + \delta_S + \delta_{Xe-Xe} + \delta_E + \delta_M + \delta_{SAS}$$

δ_0 represents the chemical shift of gaseous xenon at zero pressure taken as reference; therefore $\delta_0 = 0$.

δ_S expresses the Xe-wall interaction. In the absence of strong adsorption sites it can be obtained by extrapolation of the $\delta = f(n)$ plot to zero concentration. Fraissard et al. [55,56] have shown that there is an empirical relationship between δ_S and the mean free path, l, of the xenon imposed by the zeolite structure, this path depending on the dimensions of the channels and cages and on the ease of diffusion of the atoms. Derouane and Nagy [57] demonstrated that δ_S can also be correlated, especially at low temperature, with the effects of curvature of the internal surface influencing the physisorption energy.

δ_{Xe-Xe} corresponds to the chemical shift due to Xe–Xe interactions. This term predominates at high pressure.

δ_E and δ_M express the contributions of the electric and (in some cases) magnetic fields created by the compensating cations. For small alkaline cations, Na^+ and Li^+, and also for H^+, δ_M is zero and δ_E is negligible at ambient temperature. For example, for NaY δ varies by 4 ppm when Si/Al goes from 2.4 to 54.2 [53,54].

δ_{SAS} expresses the contribution of strong adsorption sites in the pores; they interact more strongly with the xenon atoms than does the surface of the cages and channels, leading to an increase in the chemical shift, mainly at low pressure, and to the appearance of a minimum in the $\delta = f(n)$ plot. This feature can be characterised by three parameters:

$\delta_{n\to 0}$ which is the chemical shift obtained by extrapolation of the $\delta = f(n)$ curve to zero pressure (or concentration). It depends on the nature and the number of strong adsorption sites [58,60]. This term is generally difficult to determine precisely; for this reason another parameter has been defined.

$\delta_{AS\to 0}$ which is the chemical shift obtained by extrapolation of the asymptote of the $\delta = f(n)$ curve to zero pressure (or concentration). It depends on the Xe–surface interactions, but particularly on the presence of strong adsorption sites. When the $\delta = f(n)$ plot is a straight line, $\delta_{n\to 0} = \delta_{AS\to 0}$.

$d\delta/dn$, the slope of the straight section of the plot; in the case of an isotropic Xe distribution (large cavities, Y) this is inversely proportional to the free volume of the cavities accessible to the xenon atoms.

5.1. Y zeolite.

This technique was first applied to the study of coking by Ito et al. [15]. They examined various samples of HY zeolite coked by hexane or propene cracking. The results depend on the reactant used. At relatively low n-hexane coke content (5% w/w) the slope of the $\delta = f(n)$ curve is practically the same as that of the initial zeolite. However, the increase in $\delta_{AS\to 0}$ indicates a decrease in the diffusion of xenon from one supercage to another which proves that most of the coke is located at the windows between the supercages. When there is a lot of coke (15 and 33%) for the sample coked with propene, the values of $\delta_{AS\to 0}$ and the slopes of the $\delta = f(n)$ curves increase markedly compared to the initial zeolite; the higher the coke content, the more they increase (Fig. 16). According to the ratios of the slopes of the coked samples to the initial samples, the volume accessible to xenon has decreased by 52 and 90% for the 15 and 33% coked samples, respectively. The authors deduce from this that not only the pore volume has decreased but part of the coke is located on the external surface of the crystallites and obstructs access to the supercages. This last conclusion is confirmed by the spectrum of the 33% coke sample which comprises two peaks (Fig. 17): one, very broad and very shifted, is attributed to xenon atoms adsorbed in the supercages linked with coke; the other, at 10 ppm, independent of the pressure, to those adsorbed in the mesopores

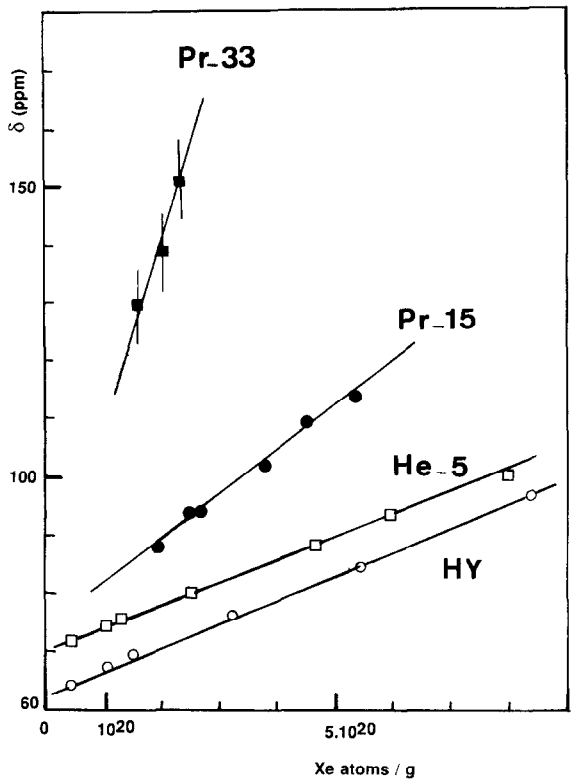

Fig. 16. 129-Xe NMR chemical shift as a function of sorbed Xe of coked HY zeolites. HY: fresh sample; He-5: 5% coke formed during hexane cracking. Pr-15 and Pr-33: 15% and 33% coke formed during propylene cracking. (from [15]).

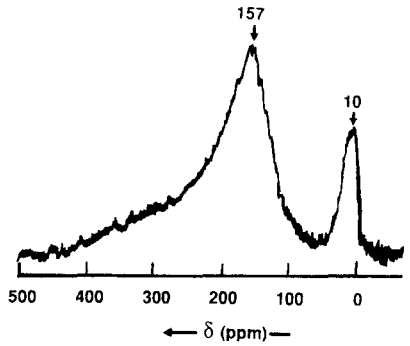

Fig. 17. 129-Xe NMR spectrum of HY zeolite coked by propylene cracking (Pr-33). P_{Xe} = 937 Torr (from [15]).

or 'microcavities' formed by the coke between the zeolite crystallites.

A more complete study was performed by Barrage et al. [8,59] for HY zeolite coked by n-heptane cracking. At low Xe concentration the initial sample presents a minimum which is more or less pronounced depending on the temperature (Fig. 18); this is characteristic of strong adsorption sites and is attributed, in agreement with the ^{27}Al–NMR spectra, to extraframework Al species (Al_{NF}). On the other hand the $\delta = f(n)$ plots for samples coked to 3, 10.5 and 15% are linear over the whole concentration range, whatever the experiment temperature (Fig. 19). This shows that the coke is deposited first of all on or close to the Al_{NF} species, thus masking the interactions between them and the xenon atoms. At the same time, HY zeolites lose more than half their activity in heptane cracking when the coke content reaches 3% [4]. This shows that the Al_{NF} species play a dominant role in the cracking activity of these zeolites at the beginning of the reaction, as has been established by various authors [61–63]; subsequently, these sites are rapidly poisoned.

Thus, for the 3% coked samples (Fig. 20-A) $\delta_{AS\to 0}$ and the slope $d\delta/dn$ depend on the temperature. For each experiment temperature the slope of $\delta = f(n)$ is close to that of the straight section of the plot for the reference sample, while the value of $\delta_{AS\to 0}$ is higher; the free volume is therefore hardly affected but xenon diffusion is restricted. The authors conclude that the coke is located initially at the windows between the supercages.

At higher coke content (10.5%) the values of $\delta_{AS\to 0}$ and the slope become independent of the

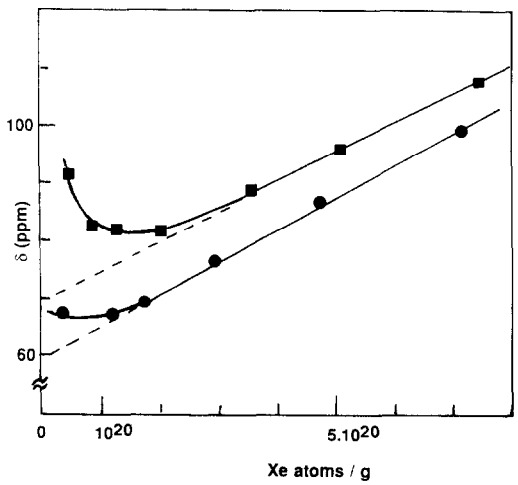

Fig. 18. 129-Xe NMR chemical shift as a function of sorbed Xe of dealuminated HY zeolites. (■) Adsorption temperature = 273 K; (●) adsorption temperature = 300 K.

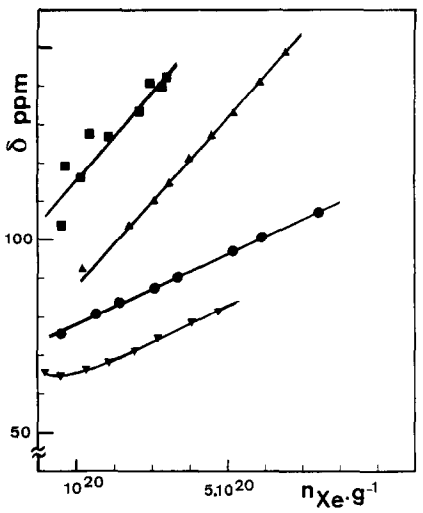

Fig. 19. 129-Xe NMR chemical shift as a function of sorbed Xe of dealuminated HY zeolites at 300 K: (▼) fresh sample; (●) 3% coked sample; (▲) 10.5% coked sample; (■) 15% coked sample (from [8]).

adsorption temperature (Fig. 20-B). Consequently, the residual internal volume can be considered as a structure of channels whose diameter is close to that of the xenon atom [64,65]. This result is confirmed by the evolution of the adsorption isotherms and the ratio of the slopes of the coked and initial samples: the free volume accessible to the xenon is divided by a factor of 2.4, the size of the cavities still accessible to xenon being then of the same order of magnitude as that of the xenon atom.

Furthermore, comparison of sample coked to 3% and to 10.5% for a given temperature (Fig. 19) shows that the slope increases markedly (multiplied by 2.4) and that $\delta_{AS\to 0}$ increases somewhat less. The authors deduce from this that the once the strong adsorption sites are covered with coke, the coke forms more homogeneously, affecting the windows as well as the free volume of the supercages.

At very high coke content (15%) (Fig. 19) the slope is identical to that of the 10.5% coked sample but the marked increase in $\delta_{AS\to 0}$ indicates that the mean free path of the xenon is smaller; xenon diffusion is then restricted, many of the cavities being therefore blocked by coke. The identity of the slopes $d\delta/dn$ for the 10.5 and 15% coked samples proves that the coke affects mainly the external surface of the crystallites. This interpretation is confirmed by the spectrum of the 15% coked sample which at high pressure comprises three signals: one broad and very shifted, corresponding to xenon atoms adsorbed in the residual internal volume; the component at 44 ppm, independent of the equilibrium pressure, is attributed to xenon adsorbed in the cavities of coke formed outside the crystallites. Finally, the signal at about 0 ppm observed at relatively high pressure is attributed to gaseous xenon whose relaxation time has been considerably reduced by the presence of paramagnetic centres due to the external coke.

Miller et al. [66] have also studied the phenomenon of coking by ^{129}Xe-NMR and by adsorption of Ar in quasi-equilibrium on HY zeolites coked with propene at 523 and 748 K. They measured the microporous volume of the zeolites by adsorption of nitrogen at 77 K and plotted the curves of δ_S, the value of the chemical shift at zero Xe con-

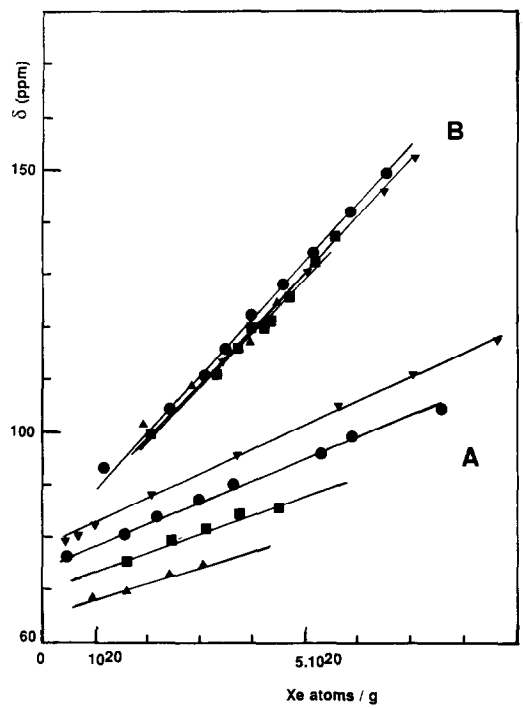

Fig. 20. 129-Xe NMR chemical shift as a function of sorbed Xe of dealuminated HY zeolites. (A) 3% coked sample; (B) 10.5% coked sample. (▼) 273 K; (●) 300 K; (■) 319 K; (▲) 338 K (adapted from [8]).

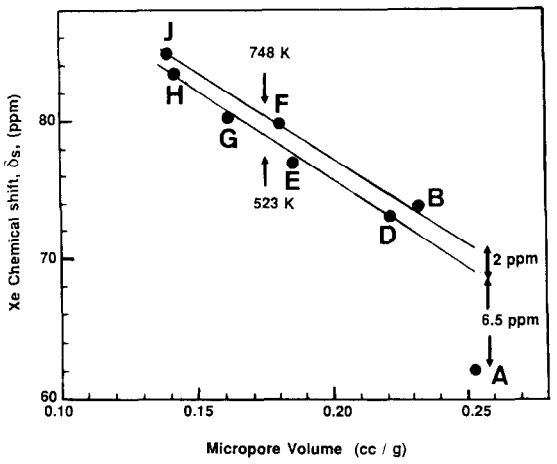

Fig. 21. 129-Xe chemical shift (zero Xe/α cage) versus N_2 micropore volume. A: 0% C ; B: 2.44% C; D: 3.45% C; E: 5.60% C; F: 7.44% C; G: 8.06% C; H: 8.38% C; J: 10.28% C (% C measured by ^{13}C NMR). (from [66]).

centration, against the microporous volume (Fig. 21). For the coked zeolites these plots are straight lines at both reaction temperatures; at a given temperature δ_S increases linearly when the microporous volume decreases, in agreement with classical results [8]. Moreover, at constant pore volume (0.25 $cm^3\ g^{-1}$) δ_S increases by 7 ppm (748 K) relative to the non-coked zeolite. Now, the ^{13}C-NMR results show that the aromaticity of the coke increases with the reaction temperature. The authors conclude from this that the shift, δ_S, is affected by the coke composition, increasing with its aromaticity.

Furthermore, the results obtained from the physisorption of Ar at 87 K show that there are two porous environments at high coke content ($>7\%$): one with coke and one without or with very little coke. These two environments are not observed by ^{129}Xe NMR at 298 K. The authors deduce that the adsorbed xenon exchanges rapidly between the two sites and, therefore, that the distance between them is small, because they are distributed homogeneously throughout the zeolite crystallites.

Bonardet et al. [45] studied the regeneration of HY zeolites, steamed and washed, then coked by ortho-xylene or n-hexane cracking. The carbonaceous residues were oxidised in several stages (in pure oxygen 8 l/h) at 573, 623 or 723 K (partial or total).

For the sample coked by *ortho*-xylene (8.7% coke), after elimination of about 45% of the coke the slope of the $\delta = f(n)$ curve is the same as that of the initial coked sample and the $\delta_{AS\to 0}$ values are barely different (Fig. 22). This first step therefore eliminates mostly external coke blocking the pore openings. This interpretation is confirmed by the fact that the two samples adsorb quasi-identical amounts of Xe at saturation.

After a second oxidation step (elimination of 82% of the initial coke) the slope $d\delta/dn$ returns to the value of the non-coked sample (Fig. 22), which proves that the free volume has been restored in this step, as is confirmed by the large increase in the amount of xenon adsorbed at saturation. However, the value of $\delta_{AS\to 0}$ (75 ppm) remains much greater than that of the non-coked sample (60 ppm) and the curvature of $\delta = f(n)$ observed at low xenon concentration for the initial sample does not appear. The authors deduce from this that the residual internal coke, more difficult to oxidise, is located at the windows between the

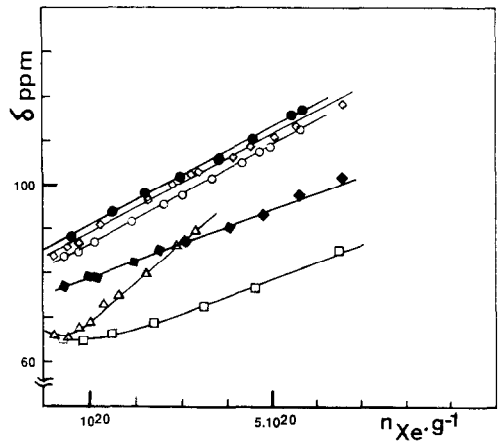

Fig. 22. 129-Xe NMR chemical shift as a function of sorbed Xe of dealuminated HY zeolites.coked during ortho-xylene cracking then partially and totally reoxidised. (□) fresh sample; (●) 8.7% coke; (◇) pyrolysed; (○) oxidized, 4.8% coke; (◆) oxidized, 1.6% coke; (■) oxidized, 0% coke (from [45]).

supercages on the extraframework aluminium species.

The last oxidation step completely eliminates the residual coke, the value of $\delta_{AS\rightarrow 0}$ being then equal to that of the initial non-coked sample. However, the slope of the linear section of the plot (Fig. 22) is multiplied by 2.3 and the amounts of xenon adsorbed at saturation are divided by 2. The internal microporous volume is therefore divided by the same factor. Moreover, the curvature of $\delta = f(n)$ at low xenon concentration is enhanced relative to that of the initial non-coked sample. Oxidation therefore causes further dealumination of the lattice, which tends to prove that coking makes certain lattice Al atoms fragile, as was established previously by ^{27}Al-NMR MAS [42]. In conclusion, complete oxidation of the coked sample creates defects in the pore structure and/or makes the lattice partially amorphous, despite the relatively mild experimental conditions employed.

The same phenomena arise, but are less pronounced, for the samples coked by n-hexane cracking.

5.2. ZSM-5 zeolite.

Other authors have investigated the coking of H-ZSM-5 zeolites. Barrage et al. [67] show that for samples of this type of zeolite in the form of pellets with alumina as binder (50-50%) and coked by methanol conversion at 670 K under nitrogen (7% coke) or hydrogen (14%) (the reaction was stopped when the dimethyl ether concentration exceeded 5% and the coke content then measured). The $\delta = f(n)$ plots are rectilinear and parallel, whereas for the initial non-coked sample this plot presents a break at about 3×10^{20} Xe/g (Fig. 23), generally attributed to the possibility of multiple collisions between the xenon atoms at the channel intersections when the Xe concentration is sufficiently high [69]. These authors conclude from this that the carbonaceous residues are probably deposited near the channel intersections.

Furthermore, the value of the slopes $d\delta/dn$, which are equal for the 7 and 14% coked samples

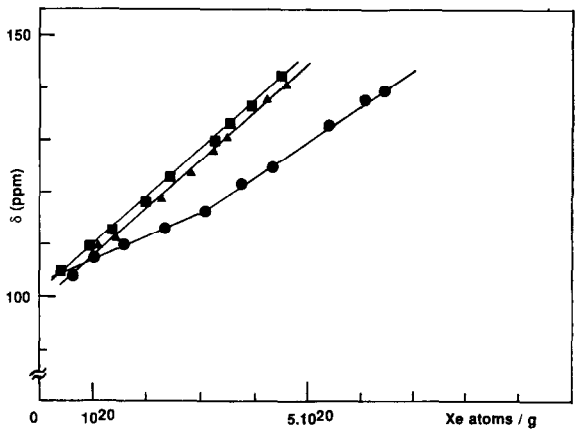

Fig. 23. 129-Xe NMR chemical shift as a function of sorbed Xe. (●) fresh H-ZSM-5 catalyst; (▲) coked in nitrogen (7% coke); (■) coked in hydrogen (14% coke) (from [67]).

(Fig. 23), made that the internal microporous volume is the same, as is confirmed by the evolution of the adsorption isotherm which are superimposed at high Xe pressure. However, the slopes are greater than that of the initial sample (multiplied by 1.35), which corresponds to a 27% loss of internal volume. This result is confirmed by the adsorption isotherms at saturation. This decrease is independent of the final coke content (7 or 14%). The authors deduce from this that when there is more than 7% of coke, the coke is deposited mainly on the outside of the crystallites. It is not detected by NMR, probably because of its nonporous structure and its distribution on the external surface of the zeolite.

Tsiao et al. [70] obtained similar results. The carbonaceous deposits on a H-ZSM-5 zeolite coked by 2 butane cracking are formed at the intersections of straight or zig-zag channels, and on the external surface of the crystallites. They suggest that the Brønsted sites are located on or near the channel intersections.

Bonardet et al. [68] investigated a H-ZSM-5 zeolite coked by acetone conversion, then regenerated either by pyrolysis at 873 K or under oxygen at 773 K in several stages.

The spectrum of the initial zeolite comprises two signals when the Xe concentration is less than

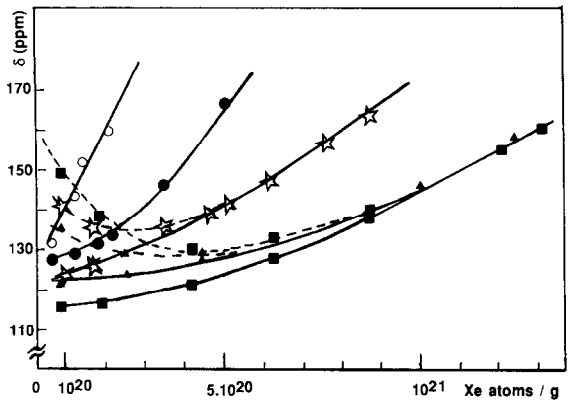

Fig. 24. 129-Xe NMR chemical shift as a function of sorbed Xe at 300 K for H-ZSM-5 zeolites coked (10.7% coke) during acetone conversion then partially decoked. (■) fresh catalyst; (○) pyrolysed sample (9.2% coke); (●) oxidized sample (9.7% coke); (★) oxidized sample (5.5% coke) (from [68]).

10^{21} at/g (Fig. 24). The presence of these two signals is due to the existence of two heterogeneous zones in the catalyst, one (signal a) behaving like a pure ZSM-5 zeolite [69] and the other (signal b) containing Al_{NF} species, which behave as strong adsorption centres at low Xe concentration. $\delta = f(n)$ plot presents a very pronounced minimum at 4.10^{20} at/g).

The sample coked to 10.7% is completely deactivated. The NMR spectrum of adsorbed xenon consists of a single signal at 10 ppm, independent of the equilibrium pressure. The authors attribute it to xenon adsorbed in the meso or the macrocavities formed by the intercrystallite coke [15].

For samples which have only been slightly regenerated, i.e., with a high residual coke (9.7% after oxidation and 9.2% after pyrolysis) only one signal is observed whatever the Xe concentration (Fig. 24). On the other hand, for samples regenerated by oxidation, containing only 5.5 and 1.5% of residual coke and for xenon concentration below 4.6×10^{20} and 5.5×10^{20} at g^{-1}, respectively, two signals are observed as for the initial zeolite (Fig. 24). The authors conclude from this that extraframework Al species are involved in the formation of coke, which is confirmed by ^{27}Al NMR [42].

They also compared the effects of pyrolysis and of oxidation. After pyrolysis or a first oxidation the samples still contain 9.2 and 9.7% of coke, respectively. However, the slope of the $\delta = f(n)$ plot is greater for the pyrolysed sample than for the oxidised sample (Fig. 24), whereas for the amount of xenon adsorbed at a given pressure it is the opposite. These results show that oxidation restores the internal volume more rapidly than pyrolysis (38 and 32%, respectively). Thus, pyrolysis eliminates first the 'light' coke compounds, whereas oxidation concerns also the polyatomatic compounds deposited on the external surface, opening the channels and allowing access to a major part of the internal volume.

Karger et al. [51] combined the ^{1}H NMR pulsed field gradient (methane as probe) and ^{129}Xe NMR of adsorbed xenon techniques to check the validity of the conclusions drawn from these two techniques. They chose an A zeolite the crystallites of which have a mean diameter of 2–3 μm (large enough to do NMR diffusion studies). This is moreover a zeolite with narrow pores and the α cages are linked by 0.42 nm diameter windows; consequently, the carbonaceous residues cannot be formed inside the crystallites. The two techniques lead to the same conclusion: the deposits of carbonaceous compounds leave the intracrystalline pore system accessible to the probe molecules more or less unchanged, while the real accessibility of the intercrystalline pore lattice is significantly reduced. They conclude from this that the carbonaceous residues are preferentially deposited on the external surface of the crystallites, which is compatible with the pore structure of A zeolite.

5.3. Conclusion

Unlike the other techniques, ^{129}Xe NMR can be used to define the location of the internal coke and its evolution with the amount of carbonaceous residue. It demonstrates the effect of zeolite structure and the nature of the reactant on coking and regeneration. It has revealed the appearance of

structure defects after total oxidation of coke in dealuminated HY zeolites.

References

[1] E.E. Wolf and F. Alfani, Catal. Rev.-Sci. Eng., 24 (1982) 329.
[2] L.D. Rollmann, J. Catal., 47 (1977) 113.
[3] L.D. Rollmann and D.E. Walsh, J. Catal., 56 (1979) 139.
[4] P. Magnoux, P. Cartraud, S. Mignard and M. Guisnet, J. Catal., 106 (1987) 235.
[5] P. Magnoux, P. Cartraud, S. Mignard and M. Guisnet, J. Catal., 106 (1987) 242.
[6] M. Guisnet and P. Magnoux, Appl. Catal., 54 (1989) 1.
[7] E.G. Derouane, Stud. Surf. Sci. Catal., 20 (1985) 221.
[8] M.C. Barrage, J.L. Bonardet and J. Fraissard, Catal. Lett., 5 (1990) 143.
[9] M. Guisnet, F.X. Cormerais, Y.S. Chen, G. Perot and E. Freund, Zeolites, 4 (1984) 108.
[10] M. Guisnet, P. Magnoux and C. Canaff, in R Setton (Ed), NATO ASI Series C, Chemical Reactions in Organic and Inorganic Constrained Systems, Vol. 165, Reidel, Dordrecht, 1985, p. 131.
[11] D.M. Bibby, N.B. Milestone, J.E. Patterson and L.P. Aldridge, J. Catal., 97 (1986) 493
[12] P. Gallezot, G. Leclercq, M. Guisnet and P. Magnoux, J. Catal., 114 (1988) 100.
[13] P. Dejaifve, A. Auroux, P.C. Gravelle, J.C. Vedrine Z. Gabelica and E.G. Derouane, J. Catal., 70 (1981) 123.
[14] D. Eisenbach and G. Gallei, J. Catal., 56 (1979) 377.
[15] T. Ito, J.L. Bonardet and J. Fraissard. J.B. Nagy, C. Andre, Z. Gabelica and E.G. Derouane. Appl. Catal., 43 (1988) L5.
[16] H. Ernst and H. Pfeifer, Z. Phys, Chem. (Leipzig), 271 (1990) 6. 1145.
[17] E.G. Derouane, J.P. Gilson and J.B. Nagy, Zeolites, 2 (1982) 42.
[18] S. Maixner, C.Y. Chen, P.J. Grobet, P.A. Jacobs and J. Weitkamp, Stud. Surf. Sci. Catal., 28 (1986) 693.
[19] P. Dejaifve, J.C. Vedrine, V. Bolis and E.G. Derouane. J. Catal., 63 (1980) 331.
[20] D.E. Walsh and L.D. Rollmann, J. Catal., 49 (1977) 369.
[21] E.G. Derouane and J.C. Vedrine, J. Mol. Catal, 8 (1980) 479.
[22] E.G. Derouane, J.P. Gilson and J.B. Nagy, J. Mol. Catal., 10 (1981) 331.
[23] J.P. Lange, A. Gutsze, J. Allgeier and H.G. Karge, Appl, Catal., 45 (1988) 345.
[24] J.L. White, N.D. Lazo, B.R. Richardson and J.F. Haw, J. Catal., 125 (1990) 260.
[25] J. Weitkamp, Stud. Surf. Sci. Catal., 5 (1980) 65.
[26] J. Weitkamp and S. Maixner, Zeolites, 7 (1987) 6.
[27] B.R. Richardson and J.F. Haw, Anal. Chem., 61 (1989) 1821.
[28] E.W. Hagaman, R.R. Chambers and M.C. Woody, Anal. Chem., 58 (1989) 387.
[29] E.J. Munson and J.F. Haw, Anal. Chem., 62 (1990) 2532.
[30] R.H. Meinhold and D.M. Bibby, Zeolites, 10 (1990) 121.
[31] G.V. Echevskii, G.V. Kharlamov, N.G. Kalinina, V.A. Poluboyarov, A.V. Pashis and V.F. Anufrienko, Kinet. Katal., 28 (6) (1987) 1456.
[32] H. Ernst, D. Freude. M. Hunger and H. Pfeifer, Stud. Surf. Sci. Catal., 65 (1991) 397.
[33] E. Brunner, H. Ernst, D. Freude, M. Hunger, C.B. Krause, D. Prager, W. Reschetilowski, W. Schwieger and K. H. Bergk, Zeolites, 9 (1989) 282.
[34] V. Bosacek, L. Kubelkova and J. Novakova, Stud. Surf. Sci. Catal., 65 (1991) 337.
[35] L. Carlton, R.G. Copperthwaite, G.J. Hutchings and C. Reynhardt, J. Chem. Soc., Chem. Commun, (1989) 1008.
[36] R.H. Meinhold and D.M. Bibby, Zeolites, 10 (1990) 146.
[37] R.H. Meinhold and D.M. Bibby, Zeolites, 10 (1990) 74.
[38] B.A. Sexton, A.E. Hughes and D.M. Bibby, J. Catal., 109 (1988) 126.
[39] D. Freude, J. Klinowski and H. Hamdan, Chem. Phys. Lett., 149 (1988) 355.
[40] G.V. Echevskii, V.M. Nekipelov, K.I. Ione and K.I. Zamaraev, React. Kinet. Catal. Lett., 33 (1) (1987) 233.
[41] K.G. Ione, V.G. Stepanov, V.M. Mastikhin and E.A. Paukshtis, Proc. 5th Int. Symp. Zeolites, Napoli, 1980, p. 223.
[42] J.L. Bonardet, M.C. Barrage and J.F. Fraissard, in R. von Ballmoss et al, (Eds), Proc. 9th Int. Zeolite Conf., Vol. II, Butterworh–Heinemann, 1993, p. 475.
[43] J.J. Fitzgerald, A. Hamza, E. Bronnimann and S.F. Dec, Solid State Ionics, 32/33 (1989) 378.
[44] P.P. Man and J. Klinowsky, Chem. Phys. Lett., 147 (1988) 581.
[45] J.L. Bonardet, M.C. Barrage and J.F. Fraissard, ACS Symp. Ser., 571 (1994) 230.
[46] H. Lechert, W.D. Basler and M. Jia, Catal. Today, 3 (1988) 23.
[47] A. de Mallman and D. Barthomeuf, Stud. Surf. Sci. Catal., 28 (1986) 609.
[48] J. Kärger, M. Hunger, D. Freude, H. Pfeifer, J. Caro, M. Bülov and H. Spindler, Catal. Today, 3 (1988) 493.
[49] J. Völter, J. Caro, M. Bülow, B. Fahlke, J. Härger and M. Hunger, Appl. Catal., 42 (1988) 15.
[50] J. Kärger, Adv. Colloid Interface Sci., 23 (1985) 129.
[51] T. Ito, J. Fraissard, J. Kärger and H. Pfeifer, Zeolites, 11 (1991) 103.
[52] T. Ito and J. Fraissard, Proc. Vth Int. Conf. Zeolites, Napoli, 1980, p. 510.
[53] J. Fraissard, T. Ito, Zeolites, 8 (1988) 350.
[54] T. Ito and J. Fraissard, J. Chem. Phys., 76 (1982) 5225.
[55] J. Demarquay and J. Fraissard, Chem. Phys. Lett., 136 (1987) 314.
[56] M.A. Springuel-Huet, J. Demarquay, T. Ito and J. Fraissard, Stud. Surf. Sci. Catal., 37 (1988) 183.
[57] E.G. Derouane and J.B. Nagy, Chem. Phys. Lett., 137 (1987) 341.
[58] T. Ito and J. Fraissard, J. Chem. Soc., Faraday Trans. 1, 83 (1987) 451.
[59] M.C. Barrage, Thesis, University. P. et M. Curie, Paris, 1992.
[60] A. Gedeon, J.L. Bonardet, T. Ito and J. Fraissard, J. Phys. Chem., 93 (1989) 2563.
[61] A. Nock and R. Rudham, Zeolites, 7 (1987) 481.
[62] U. Hammon, G.T. Kokotailo, L. Riekert and J.Q. Zhou, Zeolites, 8 (1988) 338.
[63] S.W. Addison. S. Cartlidge, D.A. Harding and G. Mc Elhiney, Appl, Catal., 45 (1988) 307.

[64] Q. Chen, Thesis, University P. et M. Curie, Paris, 1990.
[65] Q. Chen, M.A. Springuel-Huet and J. Fraissard, Stud. Surf. Sci. Catal., 65 (1991) 219i.
[66] J.T. Miller, B.L. Meyers and G.J. Ray, J. Catal., 128 (1991) 436.
[67] M.C. Barrage, F. Bauer, H. Ernst, J. Fraissard, D. Fruede and H. Pfeifer, Catal. Lett., 6 (1990) 201.
[68] J.L. Bonardet, M.C. Barrage, J.P. Fraissard, L. Kubelkova, J. Novakova, H. Ernst and D. Freude, Collect. Czech. Chem. Commun., 57 (1992) 733.
[69] Q. Chen, M.A. Springuel-Huet, J. Fraissard, M.L. Smith, D.R. Corbin and C. Dybowski, J. Phys. Chem. 96 (1992) 10914.
[70] C. Tsiao, C. Dybowski, A.M. Gaffney and J.A. Sofranko, J. Catal., 128 (1991) 520.